



A Journal of the Gesellschaft Deutscher Chemiker

Angewandte Chemie

GDCh

International Edition

www.angewandte.org

Accepted Article

Title: The crucial role of charge accumulation and spin polarization in activating carbon-based catalysts for electrocatalytic nitrogen reduction

Authors: Tao Ling, Yuanyuan Yang, Lifu Zhang, Zhenpeng Hu, Yao Zheng, Cheng Tang, Ping Chen, Ruguang Wang, Kangwen Qiu, Jing Mao, and Shi-Zhang Qiao

This manuscript has been accepted after peer review and appears as an Accepted Article online prior to editing, proofing, and formal publication of the final Version of Record (VoR). This work is currently citable by using the Digital Object Identifier (DOI) given below. The VoR will be published online in Early View as soon as possible and may be different to this Accepted Article as a result of editing. Readers should obtain the VoR from the journal website shown below when it is published to ensure accuracy of information. The authors are responsible for the content of this Accepted Article.

To be cited as: *Angew. Chem. Int. Ed.* 10.1002/anie.201915001
Angew. Chem. 10.1002/ange.201915001

Link to VoR: <http://dx.doi.org/10.1002/anie.201915001>
<http://dx.doi.org/10.1002/ange.201915001>

RESEARCH ARTICLE

The crucial role of charge accumulation and spin polarization in activating carbon-based catalysts for electrocatalytic nitrogen reduction

Yuanyuan Yang,^{[a]+} Lifu Zhang,^{[b]+} Zhenpeng Hu,^[b] Yao Zheng,^[c] Cheng Tang,^[c] Ping Chen,^[d] Ruguang Wang,^[a] Kangwen Qiu,^[a] Jing Mao,^[a] Tao Ling,^{*[a]} and Shi-Zhang Qiao^{*[a,c]}

Abstract: Cost-effective carbon-based catalysts are promising for catalyzing electrochemical N₂ reduction reaction (NRR). However, the activity origin of carbon-based catalysts towards NRR remains unclear, and regularities and rules in rational design carbon-based NRR electrocatalysts are still lacking. Here, based on a combination of theoretical calculations and experimental observations, we systematically evaluated the chalcogen/oxygen group elements (O, S, Se, and Te) doped carbon materials as potential NRR catalysts. We revealed that heteroatom-doping induced charge accumulation facilitates N₂ adsorption on carbon atom and spin polarization boosts the potential-determining step of the first protonation to form *NNH. Te and Se-doped C catalysts exhibited high intrinsic NRR activity, superior to most of metal-based catalysts. The establishing of the correlation between the electronic structure and NRR performance for carbon-based materials paves the pathway for their NRR application.

Introduction

Ammonia production plays a vital role in human society as fertilizers and chemicals.^[1] Industrial-scale ammonia synthesis is operated by the Haber-Bosch process at high temperature and pressure, which is energy-intensive and releases massive greenhouse gases.^[2] In contrast, electrochemical N₂ reduction reaction (NRR) via renewable energy to produce ammonia at ambient temperature and pressure is highly promising and attracts growing interests.^[3] Recently, great advances have been achieved in NRR, and metal,^[4] metal

carbides^[5]/nitrides^[6]/sulphide^[7]/oxides^[8] were evaluated as potential NRR active materials. However, the electrocatalytic conversion of N₂ to NH₃ is still limited by the poor production rate and unsatisfactory conversion efficiency due to the critical challenge of ultra-stable N≡N bond and competing hydrogen evolution reaction (HER).^[3] The rational design of efficient and durable electrocatalysts for NRR is still far from satisfactory.

In the past decade, carbon-based electrocatalysts have shown their great potentials in catalysing the oxygen reduction reaction (ORR),^[9] oxygen evolution reaction (OER)^[10] and HER^[11] for energy conversion and storage. Recently, heteroatom-doped carbon materials have been proved to be electroactive to reduce N₂ as well.^[12] The development of carbon-based materials with significantly improved electrocatalytic NRR activity is highly desirable due to their low-cost, environment-amity, and promising performance. However, there are still several issues unsolved: (i) the available reports on carbon-based materials for NRR are case-by-case studies and lack systematically theoretical and experimental investigations; (ii) the catalytic nature and activity origin of carbon-based catalysts towards NRR remain unclear; (iii) regularities and rules in designing efficient carbon-based NRR electrocatalysts are still not established.

Moreover, previous theoretical and experimental efforts have revealed that heteroatom-doping induced charge^[9a] and spin^[13] redistribution facilitates chemisorption of O₂, thus enhances ORR activity. According to Molecular Orbital theory, the electronic configurations of ground-state O₂ and N₂ molecules are entirely different – O₂ is spin-triplet with two unpaired electrons, whilst N₂ is diamagnetic with all electrons pair up. This may lead to different heteroatom doping induced electronic effect on NRR compared to ORR, which requires mechanistic understanding and plays crucial roles in rational design of carbon-based NRR catalysts.

Here, using metal-organic framework (MOF) derived nano porous carbon as a design platform, we theoretically and experimentally investigated the nonmetallic elements of the chalcogen/oxygen group (O, S, Se, and Te) as dopants in carbon catalysts to tune their NRR activity. We revealed that the heteroatom-doping induced charge accumulation facilitates N₂ adsorption on carbon atom and spin polarization boosts the potential-determining step of the first protonation to form *NNH; these two effects jointly contribute to overall NRR rate. With the promotion of both N₂ adsorption and *NNH formation, Se- and Te-doped C catalysts exhibited the highest NRR activity among the investigated ones. Our systematically combined computational and experimental work uncovers the catalytic nature of carbon-based materials towards NRR and paves the pathway for their future application.

[a] Y. Yang*, R. Wang, K. Qiu, Dr. J. Mao, Prof. T. Ling, Prof. S. -Z. Qiao

Key Laboratory for Advanced Ceramics and Machining Technology of Ministry of Education, Tianjin Key Laboratory of Composite and Functional Materials, School of Materials Science and Engineering, Tianjin University, Tianjin, 300072, China
Email: lingt04@tju.edu.cn

[b] L. Zhang*, Prof. Z. Hu
School of Physics, Nankai University, Tianjin 300071, China.

[c] Dr. Y. Zheng, Dr. C. Tang, Prof. S. -Z. Qiao
School of Chemical Engineering, The University of Adelaide, Adelaide, SA 5005, Australia
Email: s.qiao@adelaide.edu.au

[d] Prof. P. Chen
School of Chemistry and Chemical Engineering, Anhui University, Hefei 230000, China.

[+] These two authors contribute equally to this work.

RESEARCH ARTICLE

Results and Discussion

In this work, chalcogen/oxygen group elements, O, S, Se, and Te, were chosen to comprehensively explore the doping effect on the NRR activity of carbon-based materials. Firstly, DFT calculations were performed to evaluate the NRR activity of these catalysts. We screened possible atom sites, and found that the carbon atom adjacent to the dopant is the active site for NRR (Figures S1-S8 and Note S1). Primarily, the adsorption energy of N_2 on these catalysts (ΔE_{N_2}) was computed because the N_2 adsorption is the first step to initialize the NRR, playing an important role in the subsequent reaction pathway. ΔE_{N_2} on these catalysts is in the following order: pristine C (-0.009 eV) \approx O-doped C (-0.002 eV) $<$

S-doped C (-0.121 eV) $<$ Se-doped C (-0.275 eV) $<$ Te-doped C (-0.568 eV) (Figure 1a). To gain further insight, Bader charges of pristine and doped C were analysed. As shown in Figure 1b, the high electronegativity of O ($\chi_O = 3.5$) results in an accumulation of electrons from nearby carbon atoms ($\chi_C = 2.5$), and introduces a net positive charge on its neighbouring carbon atom. In contrast, S ($\chi_S = 2.5$), Se ($\chi_{Se} = 2.4$) and Te ($\chi_{Te} = 2.1$) create a net negative charge on their adjacent carbon atoms. Our computational results reveal that N_2 molecule barely adsorbs on carbon atom of pristine and O-doped C with $\Delta E_{N_2} \approx 0$ eV. In contrast, the N_2 adsorption is greatly enhanced on S-, Se-, and Te-doped C with charge enriched carbon atom (Figure 1b). Therefore, charge accumulation on carbon atom plays a significant role for N_2 adsorption.

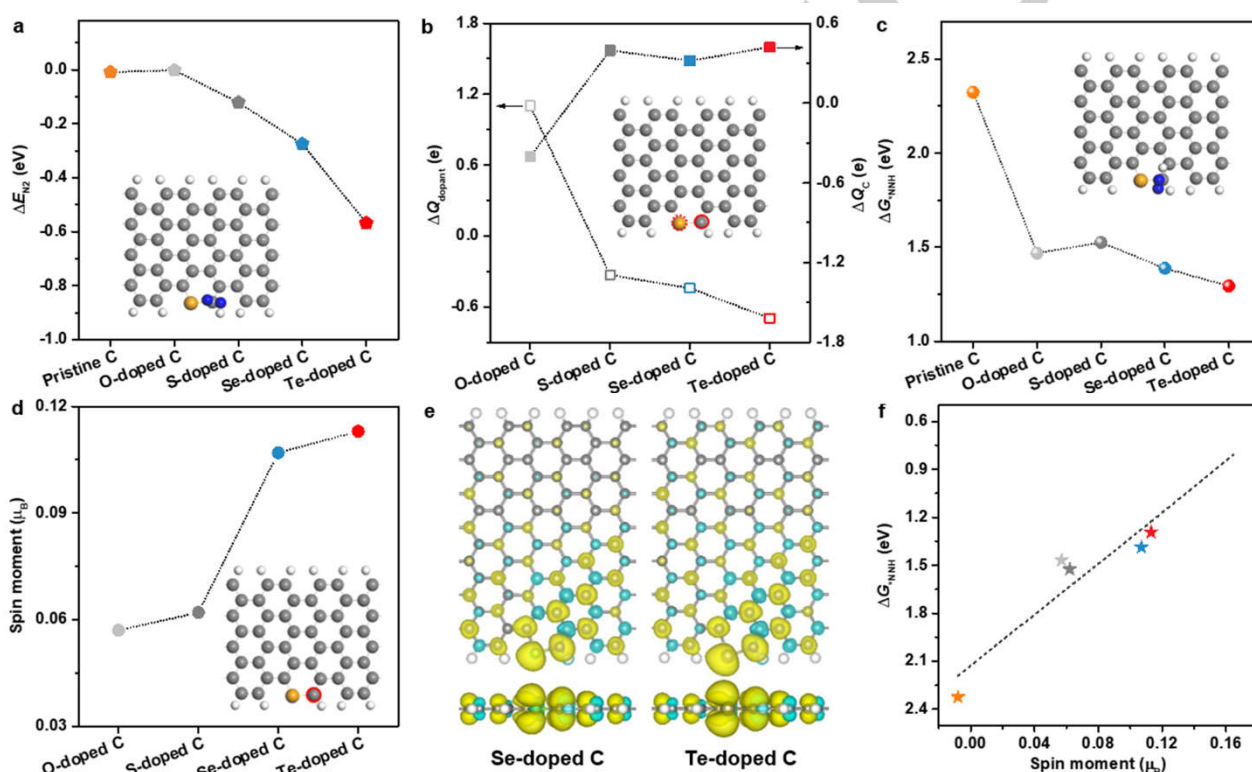


Figure 1. Physical origin of NRR on pristine and heteroatom-doped C. (a) Adsorption free energy of N_2 (ΔE_{N_2}) on pristine and heteroatom-doped C catalysts. (b) Bader charge ΔQ_{dopant} and ΔQ_C for the circled dopant atom and the circled carbon atom (neighbouring the dopant), respectively, in various heteroatom-doped C catalysts. The positive and negative charge values indicate the electron gain and loss, respectively. (c) Gibbs free energy for the formation of $*NNH$ (ΔG_{*NNH}) on pristine and heteroatom-doped C catalysts. (d) Spin moment of the carbon atom adjacent to the dopant, which is circled in the inset. (e) Top and side views of isosurface of the spin-resolved density pictures of Se- and Te-doped C. The isosurface value is set to be $0.0005 \text{ e } \text{\AA}^{-3}$. (f) The correlation between ΔG_{*NNH} and the spin moment of the active carbon atom.

The weak N_2 adsorption on pristine C leads to a high Gibbs free energy for the first protonation to form NNH^* ($\Delta G_{*NNH} = 2.32$ eV). As illustrated in Figure 1c, ΔG_{*NNH} on these catalysts follows the order: pristine C (2.32 eV) $>$ O-doped C (1.47 eV) \approx S-doped C (1.53 eV) $>$ Se-doped C (1.38 eV) $>$ Te-doped C (1.29 eV). Notably, O-doped and S-doped C with deficient and enriched charge as compared to pristine C, respectively, exhibit very similar ΔG_{*NNH} , therefore charge accumulation does not significantly affect $*NNH$ formation. To uncover the underlying mechanism, the spin distributions on pristine and doped C were calculated (Figure 1d). It should be mentioned that the carbon atoms in pristine C are not magnetic with negligible spin moment

(Figure S9). However, this value dramatically increases to 0.057, 0.062, 0.107, and 0.113 μ_B after O, S, Se, and Te doping, respectively. To further clarify such spin polarization effect, the top and side views of the spin-resolved density of doped substrates are presented in Figure 1e and Figure S10. As shown, O, S, Se and Te dopants induce the distributing of 'spin clouds' at the vicinity of adjacent carbon atoms, which are responsible for the facilitated $*NNH$ formation.^[14] It is found that there is a linear correlation between the spin moment and ΔG_{*NNH} (Figure 1f). This gives a quantitative explanation of the role of spin

RESEARCH ARTICLE

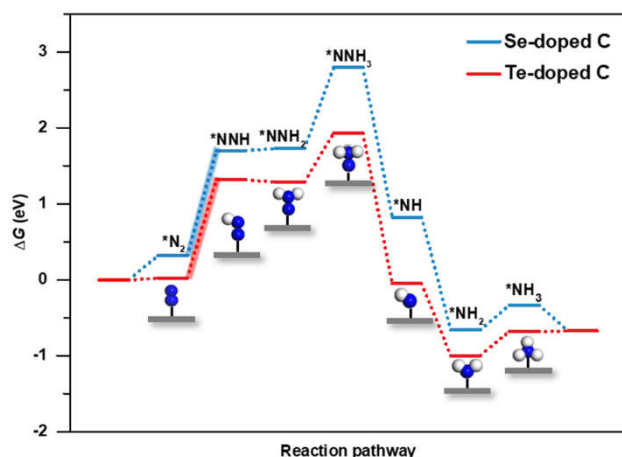


Figure 2. Free energy diagrams of the N_2 electrochemical reduction with an associative distal pathway on Se- and Te-doped C catalysts.

polarization in determining the energy barrier of the first protonation step. Noticing that previous works have demonstrated

that spin localization on carbon atoms can enhance the adsorption of O_2 ,^[13,15] thus boost ORR activity. It is reasonable that ground-state O_2 molecule is spin-triplet with two unpaired electrons, thus spin polarization on carbon atom favours O_2 adsorption. In the case of NRR, N_2 is diamagnetic molecule with all electrons pair up. Therefore, spin polarization has no obvious effect on N_2 adsorption, but on $*NNH$ formation. This was supported by the evidence that O-doped C with polarized spin density, however affords $\Delta E_{N_2} \approx 0$ eV (**Figure 1a**).

Of particular interest is that compared with O- and S-doped C, Se- and Te-doped C exhibit larger amounts of enriched charge and polarized spin moments on the active centres, suggesting their better activity towards NRR. To gain details about the conversion of the activated N_2 to NH_3 on these two catalysts, their free energy diagrams were computed. The NRR was considered through an associative distal pathway with reaction intermediates $*NNH$, $*NNH_2$, $*N$, $*NH$, and $*NH_2$ (**Figure S11**). As noted before, for pristine C, the first protonation step to form $*NNH$ is the potential-determining step with a high ΔG_{*NNH} of 2.32 eV. In the case of Se- and Te-doped C, although the first protonation step is still endergonic and potential-determining, the value of ΔG_{*NNH} is significantly reduced to 1.38 and 1.29 eV, respectively (**Figure 2**).

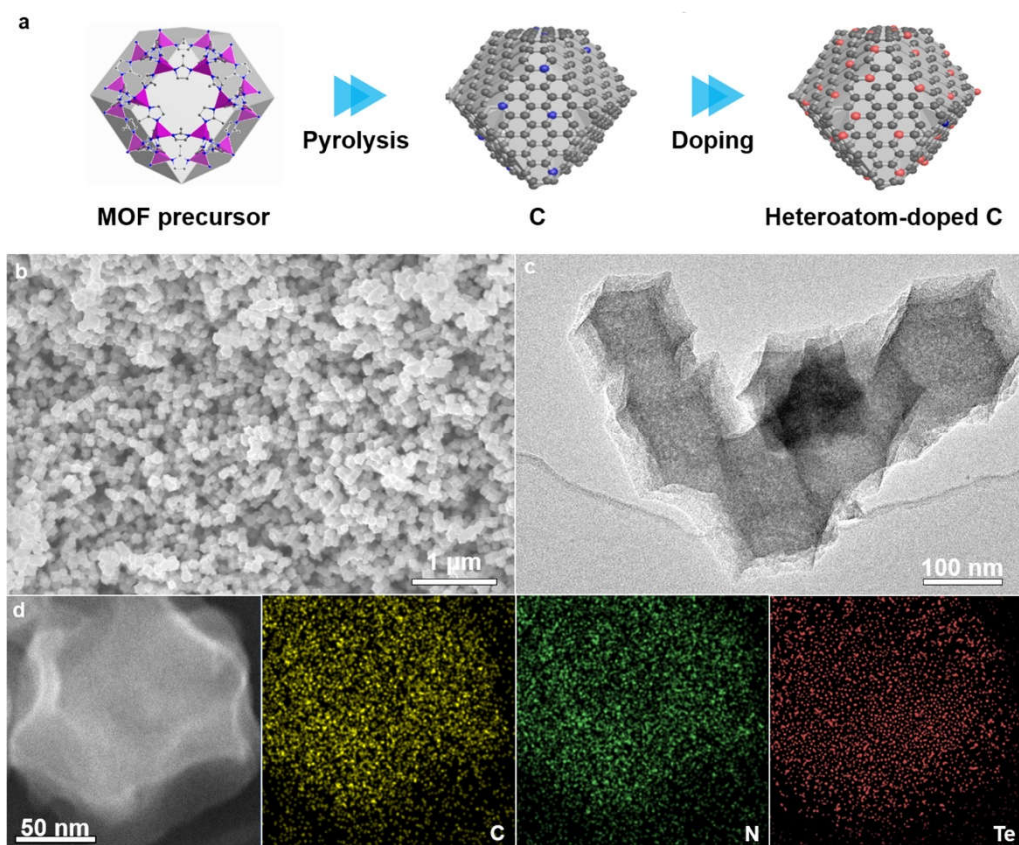


Figure 3. Characterization of heteroatom-doped C. (a) Schematic illustration of the synthetic procedure for heteroatom-doped C. (b) and (c) Scanning electron microscopic (SEM) and transmission electron microscopic (TEM) images of heteroatom-doped C, respectively. (d) HAADF-STEM image and corresponding EDS mapping results of C, N, and doping elements. The catalyst characterized here is Te-doped C.

Undoubtedly, the remarkably decreased energy barrier in the potential-determining step assures Se- and Te-doped C with greatly enhanced NRR activity.

Guided by above theoretical predictions, we experimentally attempted to fabricate O-, S-, Se- and Te-doped C, using MOF

derived nanoporous carbon as a design platform (**Figure 3a**). As shown in **Figure S12**, the derived carbon exhibits rhombododecahedral structure with an average size of 100 nm. X-ray powder diffraction (XRD) and high-resolution transmission electron microscopy (HRTEM) characterizations indicate the

RESEARCH ARTICLE

crystalline nature of small-sized graphitic carbon in as-derived carbon material (Figures S13 and S14). The broad D band in Raman spectrum (Figure S15) reveals the existence of large amounts of defects in as-derived carbon, which is beneficial for heteroatom-doping.

The incorporation of heteroatoms in as-derived carbon was realized via high-temperature processing in dopant vapor (Figure S16). The dopant concentration can be easily tuned by controlling the processing temperature (Table S1). As shown in Figure 3b and 3c, the doped C maintains the rhombododecahedral structure

of the derived carbon frameworks. The high-angle annular dark-field scanning TEM (HAADF-STEM) image and corresponding energy-dispersive X-ray spectroscopy (EDS) elemental mapping present the homogeneously uniform distribution of the C, N, and dopant elements over the whole rhombododecahedron (Figure 3d and Figure S17). Notably, in these carbon frameworks, the N element is from the original MOF precursor, which is experimentally and theoretically proved to have no significant impact on the NRR performance of as-fabricated carbon-based catalysts (Figure S18).

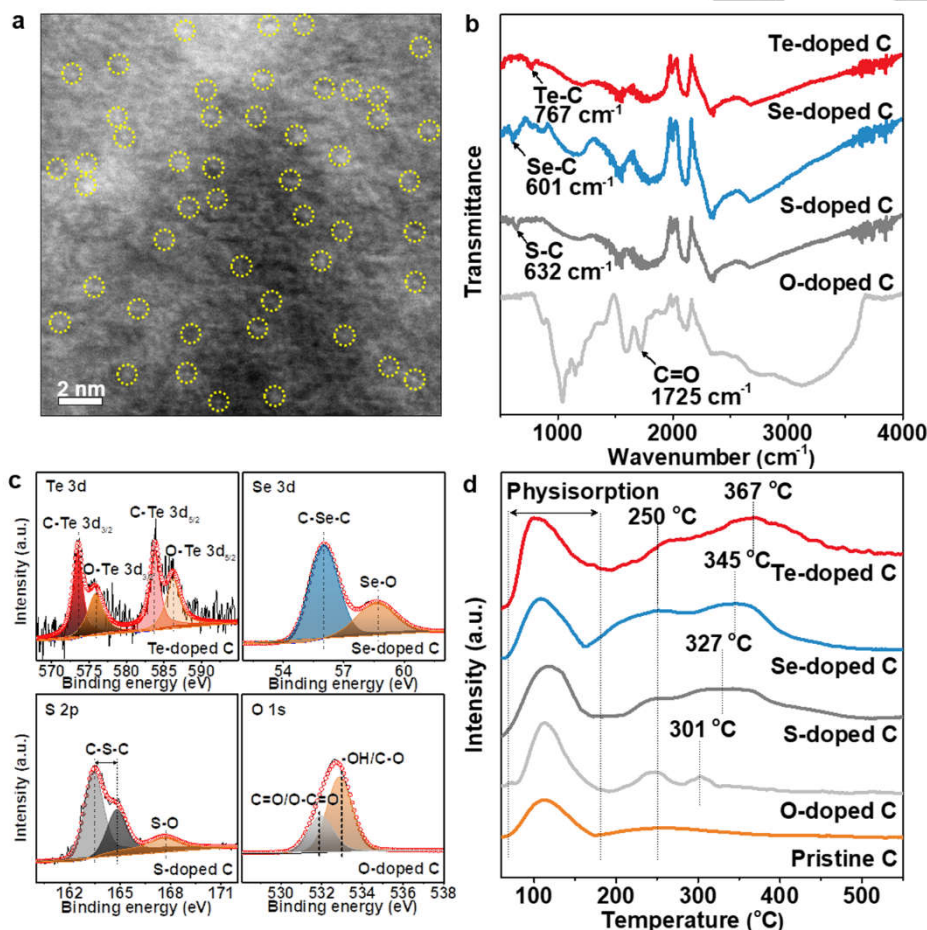


Figure 4. The chemical environment of heteroatoms in carbon frameworks. (a) HAADF-STEM image of Te-doped C catalyst. (b)-(d) FTIR, XPS and N₂-TPD spectra of O-, S-, Se-, and Te-doped C catalysts, respectively.

Furthermore, the chemical nature of heteroatom doping was investigated by a combination of HAADF-STEM, Fourier transform infrared spectroscopy (FTIR), and X-ray photoelectron spectroscopy (XPS) spectra. The atomic-level HAADF-STEM image clearly presents the individual dispersion of heteroatoms in the derived carbon (Figure 4a). In FTIR spectra, the characteristic peaks attributed to the vibrations of C=O, S-C, Se-C, and Te-C in O-, S-, Se-, and Te-doped catalysts, respectively, are clearly observed (Figure 4b). Correspondingly, the signals belonging to C=O, C-S-C, C-Se-C, and Te-C are revealed in XPS spectra for O-, S-, Se-, and Te-doped C (Figure 4c), respectively. Besides, S-O, Se-O, and Te-O signals are resolved in XPS spectra for S-, Se- and Te-doped C (Figure 4c), indicating partial oxidation of these dopants in carbon frameworks (Figure S19). These results

confirm the successful incorporation of heteroatoms in carbon frameworks.

As suggested by our calculations, the doping element governs the catalytic NRR activity of the catalysts (Figures 1 and 2). To experimentally verify the computational findings, the N₂ temperature-programmed desorption (N₂-TPD) for pristine and doped catalysts were conducted. As shown in Figure 4d, all samples exhibit a peak in the range of 70-180 °C, which can be attributed to the physical adsorption of N₂. Meanwhile, the desorption peak for chemical adsorbed N₂ is in the range of 250-400 °C, which is gradually shifted to higher temperature with larger adsorption area from pristine, through O-, S-, and Se- to Te-doped C. This indicates that the N₂ binding strength on these catalysts is in the following order: pristine C < O-doped C < S-doped C < Se-doped C < Te-doped C. This N₂-TPD result

RESEARCH ARTICLE

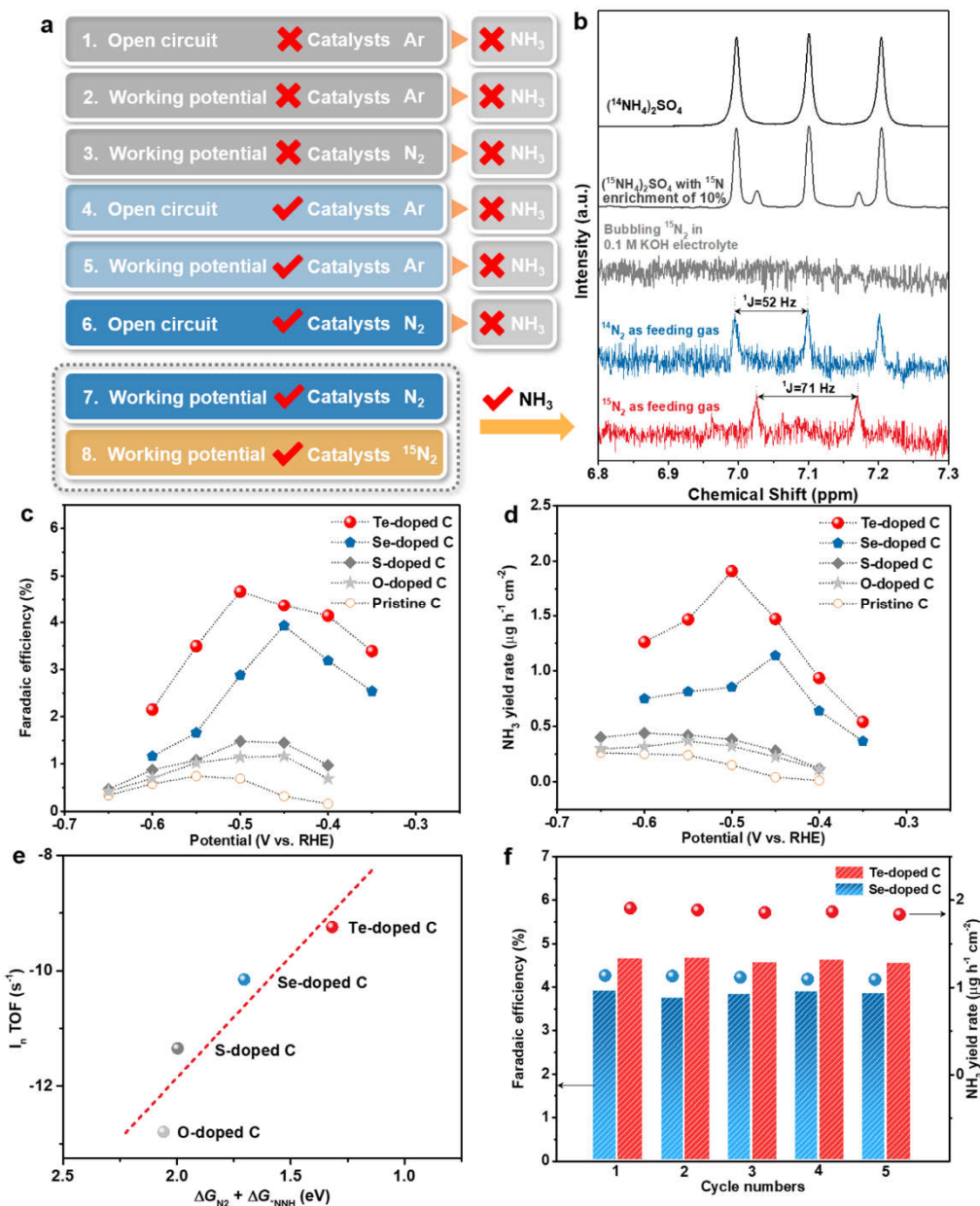


Figure 5. Experimental evaluation of NRR performance of pristine and heteroatom-doped C catalysts. (a) Flow diagram of control experiments to confirm that NH₃ production over the investigated catalysts. (b) ¹H NMR spectra (600 MHz) of standard samples of ¹⁴NH₄⁺ and ¹⁵NH₄⁺, and the electrolyte produced from the NRR reaction using ¹⁴N₂ and ¹⁵N₂ as the isotopic N₂ source. (c) and (d) Faradaic efficiency and NH₃ yield rate of pristine and heteroatom-doped C catalysts at various potentials, respectively. These experimental data were obtained using ammonia sensitive electrode method. (e) The correlation between ln(TOF) and ΔG_{N₂} + ΔG_{NH₃}. The value of TOF is the maximum for each catalyst. (f) Faradaic efficiencies and NH₃ yield rates of Se- and Te-doped C catalysts during five consecutive recycling electrolysis in N₂-saturated 0.1 M KOH. The catalysts characterized here are 11.32% O-doped C, 3.09% S-doped C, 2.74% Se-doped C, and 1.88% Te-doped C.

coincides well with the computational trend in ΔE_{N₂} for pristine and doped C catalysts (Figure 1a).

Afterwards, the electrocatalytic NRR activity of these carbon-based catalysts was experimentally evaluated using ammonia sensitive electrode^[16] in a gas-tight measurement system with a gas cleaning cell, a two-compartment cell (H-cell) separated by a proton-exchange membrane, and a gas collection cell (Figures S20-S23 and Note S2). To verify that NH₃ production was indeed produced through electrochemical N₂ reduction process over these catalysts rather than contamination, meticulous eight-step control experiments together with ¹⁵N₂

isotope labelling were carried out (Figure 5a-b, Figure S24, and Note S3).^[17] Furthermore, the NH₃ generation from the decomposition of nitrogen containing MOF-derived carbon catalysts was also carefully excluded (Figure S25).

Subsequently, the NRR activities of pristine and heteroatom-doped C catalysts with optimized dopant concentration (Figures S26 and S27) were measured in N₂-saturated 0.1 M KOH at various potentials. Their Faradaic efficiencies, NH₃ production rates and turnover frequencies (TOF, Table S1, and Note S4) are summarized in Figure 5c-e. Overall, the maximum Faradaic efficiency, NH₃ production rate, and TOF

RESEARCH ARTICLE

of these catalysts follow a similar trend: pristine C < O-doped C < S-doped C < Se-doped C < Te-doped C. This experimental observation is in excellent agreement with our computationally predicted trend in NRR activity for different dopant-incorporated carbon catalysts (**Figure 1a-b**).

As expected, Te- and Se-doped C achieve much better NRR performance than pristine, O-, and S-doped C catalysts. The Faradaic efficiency of Te- and Se-doped C catalysts reaches 4.67% @ $-0.50 V_{\text{RHE}}$ and 3.92% @ $-0.45 V_{\text{RHE}}$ (**Figure 5c**), which was 6.3 and 5.3 times, respectively, greater than the maximum value of pristine C (0.74% @ $-0.55 V_{\text{RHE}}$). Meanwhile, Te- and Se-doped C catalysts achieve the maximum average NH_3 production rates of $1.91 \mu\text{g h}^{-1} \text{cm}^{-2}$ @ $-0.50 V_{\text{RHE}}$ and $1.14 \mu\text{g h}^{-1} \text{cm}^{-2}$ @ $-0.45 V_{\text{RHE}}$, respectively (**Figure 5d**). Besides, Te- and Se-doped C exhibit excellent intrinsic activity, and their TOFs are determined to be 9.67×10^{-5} and $3.90 \times 10^{-5} \text{ s}^{-1}$, respectively (**Table S2** and **Note S4**). These values are comparable or better than those of previously reported NRR catalysts (**Table S2**).

To correlate the intrinsic NRR activity with the nature of heteroatom-doped C catalysts, the experimental TOFs are plotted as a function of their corresponding sum of Gibbs free energy for N_2 adsorption (**Figure S28**) and Gibbs free energy for the formation of *NNH ($\Delta G_{\text{N}_2} + \Delta G_{\text{NNH}}$), given that overall NRR rate on carbon materials should be governed by the coverage of adsorbed N_2 and energy barrier for *NNH formation. As shown in **Figure 5e**, a clear linear relation is observed between $\ln(\text{TOF})$ and $\Delta G_{\text{N}_2} + \Delta G_{\text{NNH}}$. Apparently, even more active carbon-based catalysts can be expected by further lowering $\Delta G_{\text{N}_2} + \Delta G_{\text{NNH}}$, which can be achieved by multiple-element doping and/or defect creating.

Finally, the long-term durability of Te- and Se-doped C catalysts were evaluated by five cycles of chronoamperometric runs, showing no obvious change in the Faradaic efficiency and the NH_3 yield rate (**Figure 5f**). Moreover, no noticeable variation of dopant content was observed after durability tests (**Table S3**). These collective results demonstrate the good stability of Te- and Se-doped C catalysts in NRR electrocatalysis.

Conclusion

In summary, we have systematically evaluated O-, S-, Se-, and Te-doped C as potential NRR catalysts based on combined theoretical and experimental investigations. We have demonstrated that the heteroatom-doping induced charge accumulation facilitates N_2 adsorption on carbon atom and spin polarization boosts the potential-determining step of the first protonation to form *NNH. We found that Se and Te dopants remarkably promote the electrocatalytic NRR activity. Our work establishes the correlation between the electronic structure and NRR performance for carbon-based materials. We believe it is helpful for future rational design of carbon-based materials towards NRR.

Acknowledgements

This work was supported by the National Outstanding Youth Science Fund Project of National Natural Science Foundation of China (51722103), the National Natural Science Foundation of China (51571149, 21576202 and 21773124), the Natural Science

Foundation of Tianjin City (19JCJQC61900), the Fok Ying Tung Education Foundation (151008), and the Fundamental Research Funds for the Central Universities Nankai University (63196010). Calculations were performed on TianHe-1A at the National Supercomputer Center, Tianjin.

Keywords: nitrogen reduction reaction • electrocatalysis • carbon materials •

- [1] a) D. Sippel, M. Rohde, J. Netzer, C. Trncik, J. Gies, K. Grunau, I. Djurdjevic, L. Decamps, S. L. A. Andrade, O. Einsle, *Science* **2018**, 359, 1484-1489; b) J. G. Chen, R. M. Crooks, L. C. Seefeldt, K. L. Bren, R. M. Bullock, M. Y. Darensbourg, P. L. Holland, B. Hoffman, M. J. Janik, A. K. Jones, M. G. Kanatzidis, P. King, K. M. Lancaster, S. V. Lymar, P. Pfromm, W. F. Schneider, R. R. Schrock, *Science* **2018**, 360, eaar6611; c) A. Good, *Science* **2018**, 359, 869-870.
- [2] a) Y. Wan, J. Xu, R. Lv, *Mater. Today* **2019**, 27, 69-90; b) C. D. Lv, C. S. Yan, G. Chen, Y. Ding, J. X. Sun, Y. S. Zhou, G. H. Yu, *Angew. Chem. Int. Ed.* **2018**, 57, 6073-6076.
- [3] a) M. A. Shipman, M. D. Szymes, *Catal. Today* **2017**, 286, 57-68; b) M. Jewess, R. H. Crabtree, *ACS Sustainable Chem. Eng.* **2016**, 4, 5855-5858; c) L. Ye, R. Nayak-Luke, R. Banares-Alcantara, E. Tsang, *Chem* **2017**, 3, 712-714; d) G. F. Chen, X. Cao, S. Wu, X. Zeng, L. X. Ding, M. Zhu, H. Wang, *J. Am. Chem. Soc.* **2017**, 139, 9771-9774; e) X. Y. Cui, C. Tang, Q. Zhang, *Adv. Energy Mater.* **2018**, 8, 25; f) C. X. Guo, J. R. Ran, A. Vasileff, S. Z. Qiao, *Energy Environ. Sci.* **2018**, 11, 45-56; g) H. P. Jia, E. A. Quadrelli, *Chem. Soc. Rev.* **2014**, 43, 547-564; h) L. L. Zhang, L. X. Ding, G. F. Chen, X. F. Yang, H. H. Wang, *Angew. Chem. Int. Ed.* **2019**, 58, 2612-2616; i) C. Tang, S.-Z. Qiao, *Chem. Soc. Rev.* **2019**, 48, 3166-3180; j) Z. Geng, Y. Liu, X. Kong, P. Li, K. Li, Z. Liu, J. Du, M. Shu, R. Si, J. Zeng, *Adv. Mater.* **2018**, 30, 1803498.
- [4] a) Z. Wang, C. Li, K. Deng, Y. Xu, H. Xue, X. Li, L. Wang, H. Wang, *ACS Sustainable Chem. Eng.* **2019**, 7, 2400-2405; b) L. L. Han, X. J. Liu, J. P. Chen, R. Q. Lin, H. X. Liu, F. Lu, S. Bak, Z. X. Liang, S. Z. Zhao, E. Stavitski, J. Luo, R. R. Adzic, H. L. L. Xin, *Angew. Chem. Int. Ed.* **2019**, 58, 2321-2325; c) Y. C. Hao, Y. Guo, L. W. Chen, M. Shu, X. Y. Wang, T. A. Bu, W. Y. Gao, N. Zhang, X. Su, X. Feng, J. W. Zhou, B. Wang, C. W. Hu, A. X. Yin, R. Si, Y. W. Zhang, C. H. Yan, *Nat. Catal.* **2019**, 2, 467-467; d) L. Hui, Y. R. Xue, H. D. Yu, Y. X. Liu, Y. Fang, C. Y. Xing, B. L. Huang, Y. L. Li, *J. Am. Chem. Soc.* **2019**, 141, 10677-10683; e) J. Wang, L. Yu, L. Hu, G. Chen, H. L. Xin, X. F. Feng, *Nat. Commun.* **2018**, 9, 7; f) Y. Yao, S. Q. Zhu, H. J. Wang, H. Li, M. H. Shao, *J. Am. Chem. Soc.* **2018**, 140, 1496-1501; g) Y. Wang, M. M. Shi, D. Bao, F. L. Meng, Q. Zhang, Y. T. Zhou, K. H. Liu, Y. Zhang, J. Z. Wang, Z. W. Chen, D. P. Liu, Z. Jiang, M. Luo, L. Gu, Q. H. Zhang, X. Z. Cao, Y. Yao, M. H. Shao, Y. Zhang, X. B. Zhang, J. G. G. Chen, J. M. Yan, Q. Jiang, *Angew. Chem. Int. Ed.* **2019**, 58, 9464-9469; [h] Z.-H. Xue, S.-N. Zhang, Y.-X. Lin, H. Su, G.-Y. Zhai, J.-T. Han, Q.-Y. Yu, X.-H. Li, M. Antonietti, J.-S. Chen, *J. Am. Chem. Soc.* **2019**, 141, 14976-14980; [i] Y.-X. Lin, S.-N. Zhang, Z.-H. Xue, J. J. Zhang, H. Su, T.-J. Zhao, G.-Y. Zhai, X.-H. Li, M. Antonietti, J.-S. Chen, *Nat. Commun.* **2019**, 10, 32.
- [5] a) L. M. Azofo, N. Li, D. R. MacFarlane, C. Sun, *Energy Environ. Sci.* **2016**, 9, 2545-2549; b) H. Cheng, L.-X. Ding, G.-F. Chen, L. Zhang, J. Xue, H. Wang, *Adv. Mater.* **2018**, 30, 1803694; c) Y. Luo, G.-F. Chen, L. Ding, X. Chen, L.-X. Ding, H. Wang, *Joule* **2019**, 3, 279-289; d) H. Cheng, P. Cui, F. Wang, L.-X. Ding, H. Wang, *Angew. Chem. Int. Ed.* **2019**, 58, 15541-15547.
- [6] a) X. Yang, J. Nash, J. Anibal, M. Dunwel, S. Kattel, E. Stavitski, K. Attenkofer, J. G. Chen, Y. Yan, B. Xu, *J. Am. Chem. Soc.* **2018**, 140, 13387-13391; b) H. Y. Jin, L. Q. Li, X. Liu, C. Tang, W. J. Xu, S. M. Chen, L. Song, Y. Zheng, S. Z. Qiao, *Adv. Mater.* **2019**, 31, 1902709.

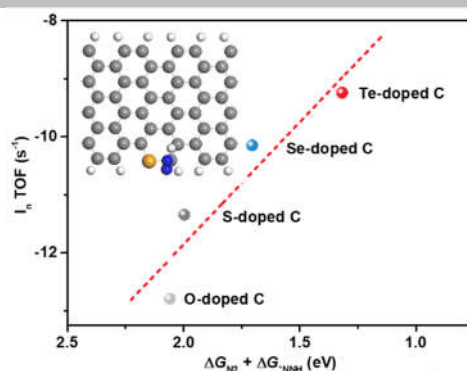
RESEARCH ARTICLE

- [7] P. Z. Chen, N. Zhang, S. B. Wang, T. P. Zhou, Y. Tong, C. C. Ao, W. S. Yan, L. D. Zhang, W. S. Chu, C. Z. Wu, Y. Xie, *Proc. Natl. Acad. Sci. USA* **2019**, *116*, 6635-6640.
- [8] L. Hu, A. Khaniya, J. Wang, G. Chen, W. E. Kaden, X. Feng, *ACS Catal.* **2018**, *8*, 9312-9319.
- [9] a) K. Gong, F. Du, Z. Xia, M. Durstock, L. Dai, *Science* **2009**, *323*, 760-764; b) Y. Zheng, Y. Jiao, L. Ge, M. Jaroniec, S. Z. Qiao, *Angew. Chem. Int. Ed.* **2013**, *52*, 3110-3116; c) Y. Jiao, Y. Zheng, M. Jaroniec, S. Z. Qiao, *J. Am. Chem. Soc.* **2014**, *136*, 4394-4403.
- [10] a) Y. Zhao, R. Nakamura, K. Kamiya, S. Nakanishi, K. Hashimoto, *Nat. Commun.* **2013**, *4*, 2390; b) J. Zhang, Z. Zhao, Z. Xia, L. Dai, *Nat. Nanotech.* **2015**, *10*, 444-452.
- [11] Y. Zheng, Y. Jiao, Y. Zhu, L. H. Li, Y. Han, Y. Chen, A. Du, M. Jaroniec, S. Z. Qiao, *Nat. Commun.* **2014**, *5*, 3783.
- [12] a) C. Lv, Y. Qian, C. Yan, Y. Ding, Y. Liu, G. Chen, G. Yu, *Angew. Chem. Int. Ed.* **2018**, *57*, 10246-10250; b) Y. Liu, Y. Su, X. Quan, X. Fan, S. Chen, H. Yu, H. Zhao, Y. Zhang, J. Zhao, *ACS Catal.* **2018**, *8*, 1186-1191; c) S. Mukherjee, D. A. Cullen, S. Karakalos, K. Liu, H. Zhang, S. Zhao, H. Xu, K. L. More, G. Wang, G. Wu, *Nano Energy* **2018**, *48*, 217-226; d) X. Yu, P. Han, Z. Wei, L. Huang, Z. Gu, S. Peng, J. Ma, G. Zheng, *Joule* **2018**, *2*, 1610-1622.
- [13] I.-Y. Jeon, S. Zhang, L. Zhang, H.-J. Choi, J.-M. Seo, Z. Xia, L. Dai, J.-B. Baek, *Adv. Mater.* **2013**, *25*, 6138-6145.
- [14] a) X. F. Li, Q. K. Li, J. Cheng, L. Liu, Q. Yan, Y. Wu, X. H. Zhang, Z. Y. Wang, Q. Qiu, Y. Luo, *J. Am. Chem. Soc.* **2016**, *138*, 8706-8709; b) X. Guo, S. Huang, *Electrochimica Acta* **2018**, *284*, 392-399.
- [15] a) L. Yang, J. Shui, L. Du, Y. Shao, J. Liu, L. Dai, Z. Hu, *Adv. Mater.* **2019**, *31*, 1804799; b) Y. Jiang, L. Yang, X. Wang, Q. Wu, J. Ma, Z. Hu, *RSC Adv.* **2016**, *6*, 48498-48503.
- [16] S. M. Chen, S. Perathoner, C. Ampelli, C. Mebrahtu, D. S. Su, G. Centi, *Angew. Chem. Int. Ed.* **2017**, *56*, 2699-2703.
- [17] a) S. Z. Andersen, V. Colic, S. Yang, J. A. Schwalbe, A. C. Nielander, J. M. McEnaney, K. Enemark-Rasmussen, J. G. Baker, A. R. Singh, B. A. Rohr, M. J. Statt, S. J. Blair, S. Mezzavilla, J. Kibsgaard, P. C. K. Vesborg, M. Cargnello, S. F. Bent, T. F. Jaramillo, I. E. L. Stephens, J. K. Nørskov, I. Chorkendorff, *Nature* **2019**, *570*, 504-508; b) G.-F. Chen, S. Ren, L. Zhang, H. Cheng, Y. Luo, K. Zhu, L.-X. Ding, H. Wang, *Small Methods* **2019**, *3*, 1800337.

RESEARCH ARTICLE

RESEARCH ARTICLE

This systematically combined computational and experimental work uncovers the catalytic nature of carbon-based materials towards electrocatalytic nitrogen reduction reaction



Yuanyuan Yang,⁺ Lifu Zhang,⁺ Zhenpeng Hu, Yao Zheng, Cheng Tang, Ping Chen, Ruguang Wang, Kangwen Qiu, Jing Mao, Tao Ling,^{*} and Shi-Zhang Qiao^{*}

The crucial role of charge accumulation and spin polarization in activating carbon-based catalysts for electrocatalytic nitrogen reduction

Accepted Manuscript